Double entropic stochastic resonance

P. S. Burada[1(a)], G. Schmid[1(b)], D. Reguera[2], J. M. Rubi[2] and P. Hänggi[1]

[1] *Institut für Physik, Universität Augsburg - Universitätsstr. 1, D-86135 Augsburg, Germany*
[2] *Departament de Física Fonamental, Facultat de Física, Universidad de Barcelona Martí i Franqués 1, E-08028 Barcelona, Spain*

Stochastic resonance (SR) is an intriguing phenomenon occurring in systems pertaining to the wide class of periodically modulated noisy systems which includes many different theoretical and experimental situations [1–10]. SR relates to a remarkable idea that changed our common perception of noise [4]: in particular, ambient noise may play a constructive role in amplifying feeble signals or may facilitate noisy transport. The phenomenon has been well studied mainly in systems having an intrinsic energetic potential whose origin is the presence of interactions. However, the prevalent role of interactions in the dynamics of a system is by no means general. It is indeed the free energy what controls the dynamics and it could happen that the entropic contribution plays a leading role. One example is the case of ion channels, where the role of entropic contributions for the phenomenon of SR has also been addressed [11–14].

Here, our focus is on stochastic resonance phenomena in confined systems, where stylized, purely geometrical constrictions may lead to a dominant entropic potential with a strong impact on the transport characteristics [15–18] that may exhibit a SR behavior in some situations [19–21].

(a) E-mail: Sekhar.Burada@physik.uni-augsburg.de
(b) E-mail: Gerhard.Schmid@physik.uni-augsburg.de

In this letter we discuss a purely entropic resonant behavior in a geometrically confined system in the presence of a longitudinal, constant bias and an oscillating force. This new resonant phenomenon is distinctly different and goes beyond the standard SR picture in several aspects. First, its origin is strictly entropic and is solely associated with geometric unevenness and confinement; in particular, there is no energetic barrier in the system. Second, the situation is characterized by the presence of two peaks in the amplification factor signaling two different optimal values of the noise strength. Finally, the enhancement of the amplification associated to the second peak is not due to noise activation, but rather is due to an optimal sensitivity of the intra-well dynamics to noise; it emerges when the entropic barrier disappears.

To illustrate this phenomenon, we consider the dynamics of a Brownian particle in the two-dimensional structure depicted in fig. 1. The time evolution of this particle, occurring in a constrained geometry subjected to a sinusoidal oscillating force $F(t)$ and a constant bias $F_{\rm b}$ acting along the longitudinal direction of the structure, can be described by means of the Langevin equation, written in the overdamped limit as

$$\gamma \frac{{\rm d}\boldsymbol{r}}{{\rm d}t} = F_{\rm b}\boldsymbol{e_x} - F(t)\,\boldsymbol{e_x} + \sqrt{\gamma k_{\rm B}T}\boldsymbol{\xi}(t), \qquad (1)$$

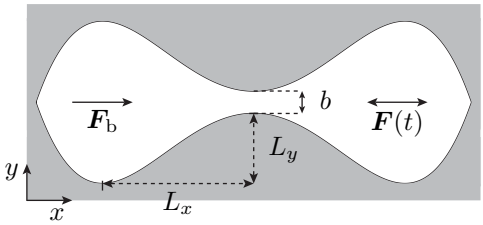

Fig. 1: Schematic illustration of the two-dimensional structure confining the motion of the Brownian particles. The symmetric structure is defined by a quartic double well function, cf. eq. (2), involving the geometrical parameters L_x, L_y and b. Brownian particles are driven by a sinusoidal force $F(t)$ and a constant bias F_b acting along the x-direction.

where $\boldsymbol{r}$ denotes the position of the particle, γ is the friction coefficient, $\boldsymbol{e_x}$ is the unit vector along the axial direction x, and $\boldsymbol{\xi}(t)$ is a Gaussian white noise with zero mean which obeys the fluctuation-dissipation relation $\langle \xi_i(t)\, \xi_j(t')\rangle = 2\,\delta_{ij}\delta(t-t')$ for $i,j = x,y$. The explicit form of the periodic input signal is given by $F(t) = A\sin(\Omega t)$, where A is the amplitude and Ω is the frequency of the sinusoidal signal. In the presence of confining boundaries, this equation has to be solved by imposing no-flow boundary conditions at the walls of the structure.

The shape of the considered 2D structure, fig. 1, which is mirror symmetric about its x- and y-axis, is defined by

$$w_{\rm l}(x) = L_y \left(\frac{x}{L_x}\right)^4 - 2\,L_y \left(\frac{x}{L_x}\right)^2 - \frac{b}{2} = -w_{\rm u}(x), \qquad (2)$$

where $w_{\rm l}$ and $w_{\rm u}$ correspond to the lower and upper boundary functions, respectively, L_x corresponds to the distance between the location of the bottleneck and that of maximal width, L_y quantifies the narrowing of the boundary functions and b is the remaining width at the bottleneck, cf. fig. 1. The local width of the structure is given by $2\,w(x) = w_{\rm u}(x) - w_{\rm l}(x)$. This particular choice of the geometry is intended to resemble the classical setup for SR, namely a double well potential, where two basins are separated by a barrier. However, we shall show that the distinct nature of this confined system, dominated by a purely entropic rather than energetic potential landscape, gives rise to new phenomena.

For the sake of simplicity, we use reduced, dimensionless units. In particular, we scale lengths by the characteristic length L_x, time by $\tau = \gamma L_x^2/k_{\rm B}T_{\rm R}$, which is the characteristic diffusion time at an arbitrary, although typical reference temperature $T_{\rm R}$, force by $F_{\rm R} = k_{\rm B}T_{\rm R}/L_x$, and frequency of the sinusoidal driving by $1/\tau$. In dimensionless form the Langevin equation (1) and the boundary functions (2) read

$$\frac{{\rm d}\boldsymbol{r}}{{\rm d}t} = F_{\rm b}\,\boldsymbol{e_x} - F(t)\,\boldsymbol{e_x} + \sqrt{D}\,\boldsymbol{\xi}(t), \qquad (3)$$

$$w_{\rm l}(x) = -w_{\rm u}(x) = -w(x) = \epsilon x^4 - 2\epsilon x^2 - b/2, \qquad (4)$$

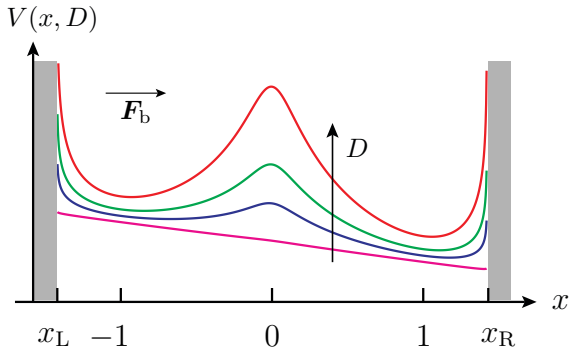

Fig. 2: (Color online) The effective one-dimensional potential $V(x,D)$, eq. (7), at a constant bias F_b and for increasing noise strength D. The aspect ratio ϵ and the bottleneck width b of the structure are set to 1/4 and 0.02, respectively. The grey shaded regions on the left and right resemble the impenetrable boundaries. The potential function diverges at $x_{\rm L}$ and $x_{\rm R}$.

where $D = T/T_{\rm R}$ is the dimensionless temperature and $\epsilon = L_y/L_x$ is the aspect ratio of the structure.

Reduction of dimensionality. – In the absence of a time-dependent applied force, *i.e.*, $F(t) = 0$, and tilting force, *i.e.*, $F_b = 0$ it has been elaborated previously [15–20,22] that the 2D Fokker-Planck dynamics corresponding to the Langevin equation (3) can be reduced to an effective 1D Fokker-Planck equation, reading in dimensionless form

$$\frac{\partial P(x,t)}{\partial t} = \frac{\partial}{\partial x}\left\{D\frac{\partial P(x,t)}{\partial x} + V'(x,D)\,P(x,t)\right\}, \qquad (5)$$

where the prime refers to the derivative with respect to x and the effective potential is given by [15,20]

$$V(x,D) = -D\,\ln[2\,w(x)]. \qquad (6)$$

This equation describes the motion of a Brownian particle in a bistable potential $V(x,D)$ of purely entropic nature. It is important to emphasize that this bistable potential was not present in the 2D Langevin dynamics, but arises due to the geometric restrictions associated to confinement. In general, the diffusion coefficient will depend on the coordinate x as well [16,17,22–24], but in the case discussed here this correction does not significantly improve the accuracy of the reduced kinetics. Therefore we do not further consider this correction. Notably, for vanishing width $2\,w(x)$ at the two opposite corners of the structure in fig. 1 this entropic potential approaches infinity, thus intrinsically accounting for a natural reflecting boundary.

In the presence of a constant bias along the x-direction of the channel the free energy becomes [15–17]

$$V(x,D) = -F_{\rm b}\,x - D\,\ln[2\,w(x)]. \qquad (7)$$

The behavior of this tilted potential is depicted in fig. 2. In contrast to the purely energetic potentials used for

classical SR [1,25], the barrier height and the shape of the potential change with noise strength D. At small D the strength of the entropic contribution is almost negligible and the potential can be approximated by $V(x,D) \approx -F_{\rm b} x$. The corresponding one-dimensional Fokker-Planck equation in the absence of periodic force reads

$$\frac{\partial P(x,t)}{\partial t} = \frac{\partial}{\partial x}\left\{ D \frac{\partial P(x,t)}{\partial x} - F_{\rm b}\, P(x,t) \right\}. \qquad (8)$$

However, in general, the potential function $V(x,D)$, eq. (7), describes a tilted bistable potential, where the height of the potential barrier depends on the noise strength D. The location of the minima also depends on the noise level, tending to a limiting value of $x = \pm 1$ for large D. More importantly, the barrier disappears and the potential does not exhibit any minima when D is smaller than a critical value D_c, which depends on the geometrical structure and on the tilt. For the shape given by eq. (2) with $\epsilon = 1/4$ and $b = 0.02$, the potential has an inflection point (*i.e.*, the barrier disappears) when $D_c \approx 0.144\, F_{\rm b}$. We will discuss below the relevance of this special situation in the context of SR.

Spectral amplification. – The response of the system to the weak periodic input signal, $F(t) = A \sin(\Omega\, t)$, is also a periodic function of time. The mean value of the position $x(t)$ in the asymptotic time limit (*i.e.*, after the memory of the initial conditions is completely lost) admits the Fourier series representation [26,27]

$$\langle x(t) \rangle_{as} = \sum_{n=-\infty}^{\infty} M_n\, e^{i\, n\, \Omega t}, \qquad (9)$$

with the complex-valued amplitudes M_n which depend nonlinearly on the driving frequency, driving amplitude and on the noise strength.

In order to study the occurrence of SR we analyzed the response of the system to the applied sinusoidal signal in terms of the spectral amplification η, which is defined as [26,27]

$$\eta = \left(\frac{2|M_1|}{A} \right)^2. \qquad (10)$$

Two-state approximation. – If the potential barrier is sufficiently high and the two basins of attraction are well separated, the intra-well motion may be neglected, and a simplified two-state description can be used to get useful insights into the full dynamics [28,29]. Within the two-state approximation the transition rate from one well to the other can be determined in terms of the mean first passage time (MFPT) [25] to reach a potential minimum starting out from the other minimum of the tilted bistable potential $V(x,D)$. Accordingly, the forward (k_+) and backward (k_-) rates are given by

$$k_\pm = \frac{1}{T_\pm(\, x_\mp \to x_\pm\,)}, \qquad (11)$$

where x_- and x_+ indicate the noise(D)-dependent location of the left and right minima, respectively; $T_+(x_- \to x_+)$ is the mean first passage time for reaching x_+ starting out at x_-; and, vice versa, $T_-(x_+ \to x_-)$ is the mean first passage time in the backward direction. More explicitly, the forward and backward mean first passage times are

$$T_+ = \frac{1}{D} \int_{x_-}^{x_+} {\rm d}x\, \frac{e^{-F_{\rm b}\, x/D}}{w(x)} \int_{x_{\rm L}}^{x} {\rm d}y\, w(y)\, e^{F_{\rm b}\, y/D}, \qquad (12)$$

and

$$T_- = \frac{1}{D} \int_{x_+}^{x_-} {\rm d}x\, \frac{e^{-F_{\rm b}\, x/D}}{w(x)} \int_{x_{\rm R}}^{x} {\rm d}y\, w(y)\, e^{F_{\rm b}\, y/D}, \qquad (13)$$

where $x_{\rm L}$ and $x_{\rm R}$ are, respectively, the left and right limiting values at which the boundary function vanishes, see fig. 2. Note that the bias $F_{\rm b}$ must be small in order to have two well-separated basins of attraction (see discussion of the potential). Within the two-state description the mean position is given by

$$q_0 = \frac{k_+ x_+ + k_- x_-}{k_+ + k_-}. \qquad (14)$$

A sinusoidal signal leads to a modulation of the barrier height of the double well potential and consequently to a modulation of the rates $k_\pm$ [28]. One obtains the spectral amplification in the lowest order of A/D, reading

$$\eta = \frac{1}{D^2} \left[\frac{(x_+ - x_-)^2\; k_+\, k_-}{k_+ + k_-} \right]^2 \frac{1}{(k_+ + k_-)^2 + \Omega^2}. \qquad (15)$$

Note that for the symmetric case, *i.e.*, $k_+ = k_- = k$ and $x_\pm = \pm 1$, the spectral amplification given in eq. (15) reduces to the well-known expression,

$$\eta = \frac{1}{D^2}\, \frac{4\, k^2}{4\, k^2 + \Omega^2}, \qquad (16)$$

which in the linear response regime is by construction independent of the amplitude strength [1,26,27,29].

1D modeling. – The two-state description of the linear response fails for either large driving amplitudes, small driving frequencies [1,30] or very weak noise [31]. In such circumstances, the 1D Fokker-Planck equation has to be considered and the nonlinear response analyzed [1,27,30,31]. In the presence of a sinusoidal signal $F(t)$ the 1D Fokker-Planck reads

$$\frac{\partial P(x,t)}{\partial t} = \frac{\partial}{\partial x}\left\{ D \frac{\partial P}{\partial x} + [V'(x,D) + F(t)]\; P \right\}. \qquad (17)$$

We have integrated numerically the above equation by spatial discretization, using a Chebyshev collocation method, and employing the method of lines to reduce the kinetic equation to a system of ordinary differential equations, which was solved using a backward differentiation formula method. Thereby we obtain the time-dependent

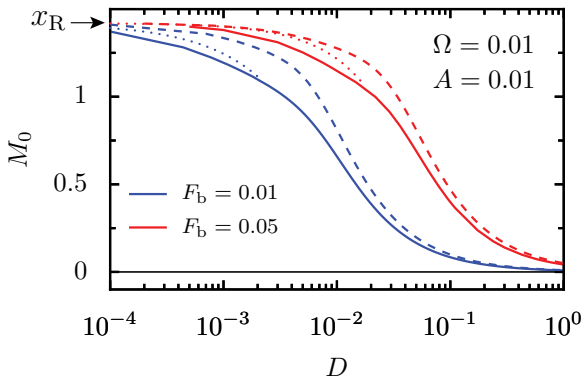

Fig. 3: (Color online) The time averaged mean position M_0 as a function of the noise strength D for different tilting force values. The solid lines correspond to the numerical integration of the 1D Fokker-Planck equation, eq. (17), and the dashed lines correspond to the two-state approximation, eq. (14), *i.e.*, $M_0 \equiv q_0$. In the potential function we set the aspect ratio $\epsilon = 1/4$ and the bottleneck width $b = 0.02$. The dotted lines represent the behavior of M_0 at small D obtained by integration of eq. (8). For the symmetric case ($F_b = 0$) all these lines collapse to the black solid line, *i.e.* $M_0 = 0$.

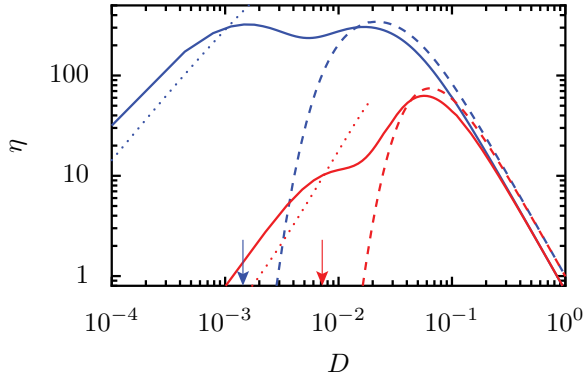

Fig. 4: (Color online) The behavior of the spectral amplification factor η as a function of the noise strength D for the same parameters as in fig. 3. The solid lines correspond to the numerical integration of the 1D Fokker-Planck equation, eq. (17), whereas the dashed lines correspond to the two-state approximation, eq. (15). The behavior of η at small D obtained by integration of eq. (8) with a periodic forcing and at the respective tilting force values is represented with dotted lines. The arrows indicate the critical value D_c that corresponds to the vanishing of the barrier.

probability distribution $P(x,t)$ and the time-dependent mean value of the position, $\langle x(t)\rangle = \int x\, P(x,t)\, \mathrm{d}x$. In the long-time limit this mean value approaches the periodicity of the input signal with angular frequency Ω, see refs. [26,27]. After a Fourier-expansion of $\langle x(t)\rangle$ one finds the time averaged mean position $M_0 = M_0(A,D)$ and amplitude $M_1 = M_1(A,D)$ of the first harmonic of the response.

The mean position M_0 as a function of the noise strength D is depicted in fig. 3 for two different tilting force values. For comparison, the approximated mean position q_0 obtained within the two-state modeling is also plotted. At very small D there is no barrier and the particle oscillates just in the vicinity of the boundary, either at x_R or x_L depending on the direction of the tilt. As the noise strength increases the barrier height increases, see fig. 2, and the inter-well (from one well to the other) dynamics become more dominant. Remarkably, the behavior of the mean position can be qualitatively captured within the two-state approximation.

For the 1D modeling the spectral amplification for the fundamental oscillation is computed accordingly, cf. eq. (10). The comparison between the results of the 1D modeling and the two-state approximation for the parameter η as a function of the noise strength D and for two different tilting force values is depicted in fig. 4. Within the 1D modeling η exhibits a double-peak behavior for a finite tilt. The appearance of the main peak at higher D, which is due to the synchronization of the periodic signal with the activated inter-well dynamics, can be nicely captured within the two-state model. However, there is a second peak at small values of noise that cannot be described within the two-state model. As it is discussed before, at small noise strengths there is no barrier and the particle oscillates in the vicinity of the boundary. As we increase the noise one can observe a steep rise in η with D which is a consequence of noise helping the particle to climb higher the potential hill (see fig. 4). The second peak at small D is attributed to the intra-well dynamics, and could also be observed for mono-stable energetic potentials [5,32,33]. The steepness of increase of η depends on the strength of the tilting force. However, beyond D_c, the barrier appears and gets higher as we increase the noise level, thus leading to a decrease in the amplification since the dynamics of the particle is now hampered by the need to overcome a barrier. Therefore, the inflection point of the effective potential —which marks the appearance of the barrier— locates the position of a new optimal regime of noise in terms of signal amplification.

2D numerical simulation. – In order to check the accuracy of the one-dimensional description we compared the obtained results with the results of Brownian dynamic simulations, performed by integrating the full overdamped Langevin equation (3). The simulations were carried out using the standard stochastic Euler-algorithm.

The behavior of the spectral amplification η as a function of the noise strength D for different tilting force values is depicted in fig. 5. It is worth to mention that the results of the 1D modeling (lines) are in very good agreement with the numerical simulations of the full 2D system (symbols) within a small relative error. As one would expect the resonant behavior is absent for zero tilting force, *i.e.*, for the purely symmetric case [20], whereas in the presence of a tilting force, the spectral amplification exhibits a double-peak structure. As discussed before, the inter-well dynamics is responsible of the appearance of the main peak

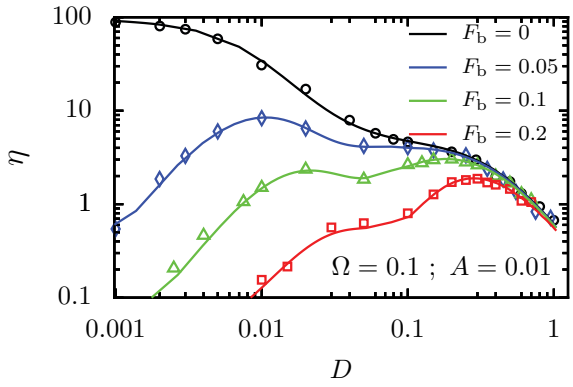

Fig. 5: (Color online) The spectral amplification η as a function of the noise strength D at various tilting force values. The lines correspond to the numerical integration of the 1D Fokker-Planck equation, eq. (17), whereas the symbols correspond to the results of the Langevin simulations for the two-dimensional structure with the shape defined by the dimensionless function $w(x) = -0.25\,x^4 + 0.5\,x^2 + 0.01$.

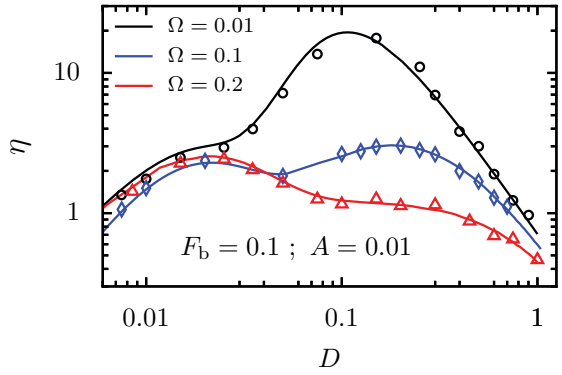

Fig. 6: (Color online) Same as in fig. 5, but for various input signal frequencies.

at higher noise strengths D whereas the second peak at smaller noise strengths is related to the disappearance of the barrier. By changing the tilt, the second peak gets shifted to higher values of noise following the predicted behavior for the inflection point, namely $D_c \approx 0.144\,F_b$.

The behavior of the spectral amplification for different frequencies is plotted in fig. 6. The height of the main peak in η at high noise strength increases as the frequency of the input signal decreases, resembling the behavior of classical SR [2]. Overall, the perfect double-peak structure in the spectral amplification is present only at moderate frequency range. A similar behavior of double-peak SR could also be observed in purely energetic systems, with a double well potential, either at high input frequencies [27,32] or at small frequencies in the presence of inertia [34].

Figure 7 depicts the behavior of the spectral amplification for different values of the amplitude of the driving force. The inter-well dynamics responsible of the appearance of the main peak in η at higher noise strengths is not much affected by the variation of the input signal

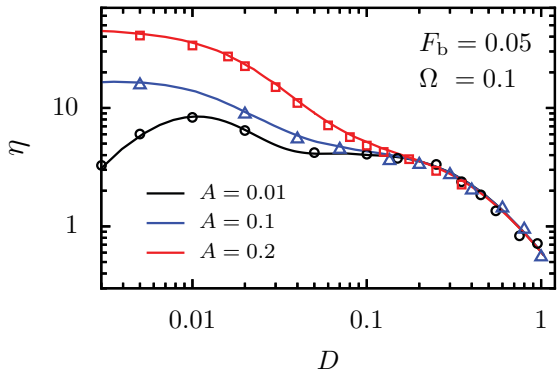

Fig. 7: (Color online) Same as in fig. 5, but for various input signal amplitudes.

amplitude. In contrast, the second peak is greatly affected by the amplitude of the input signal. A clear double-peak structure in η can be obtained only at small signal amplitudes, since when the amplitude of the forcing exceed the bias F_b, the particle can move throughout the whole structure assisted by the periodic forcing and therefore loses its sensitivity to the noise strength.

Conclusions. – In this work we have studied the influence of a constant bias on the resonant response of a geometrically constrained system. In the absence of the tilting force the system does not exhibit a SR behavior [20]. Applying a constant bias, one can bring the system to an optimal regime where it exhibits a double ESR in the spectral amplification. We want to stress that the phenomenon is strictly entropic, since there is no purely energetic barrier in the system. The ESR emerges due to the interplay between the tilt and the entropic barrier which originates in our case from the unevenness of geometrical restrictions. The double-peak behavior arises due to two different dynamic regimes: i) a regime, which is genuine of entropic systems, that occurs at high noise strengths where the main peak in the amplification is due to the synchronization of the periodic signal with noise-assisted hopping events; and ii) a regime, at low noise strengths, at which the potential has an inflection point. The system thus becoming optimally sensitive to noise. Note that noise plays a two-fold role in an entropic system: on the one hand, it facilitates the dynamics, but on the other hand it intensifies the strength of the entropic contribution leading to the appearance of barriers that hamper transport. The second peak at smaller noise intensity signals the optimum balance between these two roles. This double resonant behavior renders the possibility for complete control of the optimization of the response of a system in the presence of noise. The main peak stemming from the inter-well dynamics can be strikingly controlled by tuning the frequency, while the second peak can be controlled either by changing the strength of the tilt or the amplitude of the periodic input signal. The double resonant peak behavior is a clear

signature of the richness of dynamical behaviors in driven confined systems. The occurrence of this phenomenon depends only on a few controllable parameters that can be advantageously tuned to achieve an optimal response.

* * *

This work has been supported by the DFG via the collaborative research center, SFB-486, project A10, via the project no. 1517/26-2, the Volkswagen Foundation (project I/80424), the German Excellence Initiative via the *Nanosystems Initiative Munich* (NIM), and by the DGCyT of the Spanish government through grant No. FIS2008-04386.

REFERENCES

[1] Gammaitoni L., Hänggi P., Jung P. and Marchesoni F., *Rev. Mod. Phys.*, **70** (1998) 223.
[2] Bulsara A. R. and Gammaitoni L., *Phys. Today*, **49** (1996) 39.
[3] Hänggi P., *ChemPhysChem*, **3** (2002) 285.
[4] Gammaitoni L., Hänggi P., Jung P. and Marchesoni F., *Eur. Phys. J. B*, **69** (2009) 1.
[5] Vilar J. M. G. and Rubí J. M., *Phys. Rev. Lett.*, **77** (1996) 2863.
[6] Vilar J. M. G. and Rubí J. M., *Phys. Rev. Lett.*, **78** (1997) 2886.
[7] Anishchenko V. S., Neiman A. B., Moss F. and Schimansky-Geier L., *Phys. Usp.*, **42** (1999) 7.
[8] Schmid G., Goychuk I. and Hänggi P., *Europhys. Lett.*, **56** (2001) 22.
[9] Yasuda H., Miyaoka T., Horiguchi J., Yasuda A., Hänggi P. and Yamamoto Y., *Phys. Rev. Lett.*, **100** (2008) 118103.
[10] Murali K., Sinha S., Ditto W. L. and Bulsara A. R., *Phys. Rev. Lett.*, **102** (2009) 104101.
[11] Goychuk I. and Hänggi P., *Phys. Rev. Lett.*, **91** (2003) 070601.
[12] Goychuk I. and Hänggi P., *Phys. Rev. E*, **69** (2004) 021104.
[13] Goychuk I., Hänggi P., Vega J. L. and Miret-Artés S., *Phys. Rev. E*, **71** (2005) 061906.
[14] Parc Y. W., Koh D. and Sung W., *Eur. Phys. J. B*, **69** (2009) 127.
[15] Reguera D., Schmid G., Burada P. S., Rubí J. M., Reimann P. and Hänggi P., *Phys. Rev. Lett.*, **96** (2006) 130603.
[16] Burada P. S., Schmid G., Reguera D., Rubí J. M. and Hänggi P., *Phys. Rev. E*, **75** (2007) 051111.
[17] Burada P. S., Schmid G., Talkner P., Hänggi P., Reguera D. and Rubí J. M., *BioSystems*, **93** (2008) 16.
[18] Burada P. S., Hänggi P., Marchesoni F., Schmid G. and Talkner P., *ChemPhysChem*, **10** (2009) 45.
[19] Burada P. S., Schmid G., Reguera D., Vainstein M. H., Rubi J. M. and Hänggi P., *Phys. Rev. Lett.*, **101** (2008) 130602.
[20] Burada P. S., Schmid G., Reguera D., Rubi J. M. and Hänggi P., *Eur. Phys. J. B*, **69** (2009) 11.
[21] Borromeo M. and Marchesoni F., *Eur. Phys. J. B*, **69** (2009) 23.
[22] Zwanzig R., *J. Phys. Chem.*, **96** (1992) 3926.
[23] Reguera D. and Rubí J. M., *Phys. Rev. E*, **64** (2001) 061106.
[24] Berezhkovskii A. M., Pustovoit M. A. and Bezrukov S. M., *J. Chem. Phys.*, **126** (2007) 134706.
[25] Hänggi P., Talkner P. and Borkovec M., *Rev. Mod. Phys.*, **62** (1990) 251.
[26] Jung P. and Hänggi P., *Europhys. Lett.*, **8** (1989) 505.
[27] Jung P. and Hänggi P., *Phys. Rev. A*, **44** (1991) 8032.
[28] McNamara B. and Wiesenfeld K., *Phys. Rev. A*, **39** (1989) 4854.
[29] Jung P. and Hänggi P., *Z. Phys. B*, **90** (1993) 255.
[30] Casado-Pascual J., Gómez-Ordóñez J., Morillo M. and Hänggi P., *Europhys. Lett.*, **65** (2004) 7.
[31] Shneidman V. A., Jung P. and Hänggi P., *Phys. Rev. Lett.*, **72** (1994) 2682.
[32] Evstigneev M., Reimann P., Pankov V. and Prince R. H., *Europhys. Lett.*, **65** (2004) 7.
[33] Mayr E., Schulz M., Reineker P., Pletl T. and Chvosta P., *Phys. Rev. E*, **76** (2007) 011125.
[34] Alfonsi L., Gammaitoni L., Santucci S. and Bulsara A. R., *Phys. Rev. E*, **62** (2000) 299.